Fizika Nizkikh Temperatur, 2011, v. 37, No. 1, p. 64–70

Quantum interference effects in a system of two tunnel point-contacts in the presence of single scatterer: simulation of a double-tip STM experiment

N.V. Khotkevych and Yu.A. Kolesnichenko

B. Verkin Institute for Low Temperature Physics and Engineering of the National Academy of Sciences of Ukraine
47 Lenin Ave., Kharkov 61103, Ukraine
E-mail: Kolesnichenko@ilt.kharkov.ua

J.M. van Ruitenbeek

Kamerlingh Onnes Laboratorium, Universiteit Leiden, Postbus 9504, Leiden 2300, The Netherlands

Received October 12, 2010

The conductance of systems containing two tunnel point-contacts and a single subsurface scatterer is investigated theoretically. The problem is solved in the approximation of *s*-wave scattering giving analytical expressions for the wave functions and for the conductance of the system. Conductance oscillations resulting from the interference of electron waves passing through different contacts and their interference with the waves scattered by the defect are analyzed. The prospect for determining the depth of the impurity below the metal surface by using the dependence of the conductance as a function of the distance between the contacts is discussed. It is shown that the application of an external magnetic field results in Aharonov–Bohm type oscillations in the conductance, the period of which allows detection of the depth of the defect in a double tip STM experiment.

PACS: 61.72.J– Point defects and defect clusters;
73.63.Rt Nanoscale contact;
74.55.+v Tunneling phenomena: single particle tunneling and STM.

Keywords: magnetic field, Aharonov–Bohm oscillations, two tunnel point-contacts.

With the further development of scanning tunnelling microscopy (STM) it has become clear that a single STM probe is often not enough for obtaining information on the detailed characteristics of the surface under investigation. A logical development of the one-tip approach is a dual-tip experimental setup, which can provide us with richer information than conventional single-probe STM. Despite the apparent technical complexity of the dual-tip STM (DSTM) in comparison with standard STM several groups have demonstrated successful solutions for such refinement of the STM technology [1– 4].

DSTM can be realized in different ways. For example, it can be a spatially extended STM tip with two protrusions, each ending in a cluster or a single atom [5]. A second approach is a coaxial beetle-type double-tip STM design that looks advantageous in retaining the standard STM stability [6]. The most versatile DSTM comprises two individual tips, which can be driven independently. In this case the distance between the tips is limited in principle only by a parameter such as the characteristic tip radius [2]. Another original example of the DSTM was proposed in [7], where one contact can be created directly on the surface, while the other one was the STM-tip itself.

For DSTM experiments with two independent probes there are different possibilities for applying voltages to the tunnelling contacts. There are two basic circuit designs: in the first one electrons are emitted from the first contact and then gathered at the second, i.e., the current flows from one contact to the other through the surface being probed [8,9]. This method allows capturing a trans-conductance map, and in addition allows the implementation of three-terminal ballistic electron emission spectroscopy (BEES) without introduction of macroscopically bounded contacts [3]. In the second basic scheme proposed in Ref. 5 the bias is applied between the two tips and the sample, i.e., the current flows from two contacts into the sample.

Subsurface defects, adatoms, and steps on the metal surface result in the appearance of Friedel-like oscillations in the STM conductance $G = dI / dV$ — a nonmonotonic dependence of G with the distance between the STM tip

and the defect r_0 (for a review see [10]). The study of this dependence can be used for the detection of buried defects and for investigation of their characteristics. Methods for determining defect positions below a metal surface using a single tip STM have been proposed before: this can be achieved using the period of oscillation of the conductance as a function of bias [11,12] or by exploiting the interference pattern of conductance as a function of position, $G(r_0)$, which is very pronounced for open directions of Fermi surface [13–15]. These approaches are very suitable for the surfaces of simple metals, such as the noble metals, but application to conductors having a more complicated Fermi surface geometries will be difficult and has not yet been explored.

In the present work we examine the case of injection of electrons to the surface by the first and the second contacts simultaneously. We consider this realization of a double-tip experiment as a natural refinement of the single-tip STM problem for the study of single defects buried under the metal surface [11,12,15].

The idea of using multiple tunnelling contacts for determining the depth and location of impurities under a metal or semiconductor surface has been expressed earlier in Ref. 8. The paper by Niu et al., Ref. 8, proposes a method for determining the desired depth by measuring the transconductance between two tips of the dual-tip scanning tunneling microscope. In the present paper we propose a different approach, namely, by measuring the phase change $\Delta\vartheta$ in the conductance oscillations as a function of the distance between two STM tips *d*. Such phase changes can be measured experimentally with great precision. We show that $\Delta\vartheta$ can be expressed in terms of the distance *d* (in units of the Fermi wave vector k_F), the position of the defect in the plane parallel to surface plane ρ_0, which is easily defined experimentally, and the unknown depth of the defect z_0. Thus by measurement of $\Delta\vartheta(d)$ it is possible to determine the depth of the buried impurity. The procedure of defining z_0 is further simplified when a magnetic field **H** is applied to the system. In this case the STM conductance G undergoes Aharonov–Bohm type oscillations. These oscillations result from the quantization of the magnetic flux through the area formed by the electron trajectories from the contacts to the defect and the line connecting the contacts (Fig. 1). For a weak magnetic field the electron trajectories and the line connecting the contacts form a triangle, and from its area S the defect depth can be found easily.

As a model for the double-tip STM geometry we consider two metal half-spaces separated by an infinitely thin nonconducting interface at $z = 0$, which contains two small regions (contacts) that allow electron tunnelling (see Fig. 1). The origin of the coordinate system $\mathbf{r} = 0$ is chosen in the center of the first contact. The *x*-axis is directed along the the line connecting the contacts. For the potential barrier in the plane $z = 0$ we use the function [17]

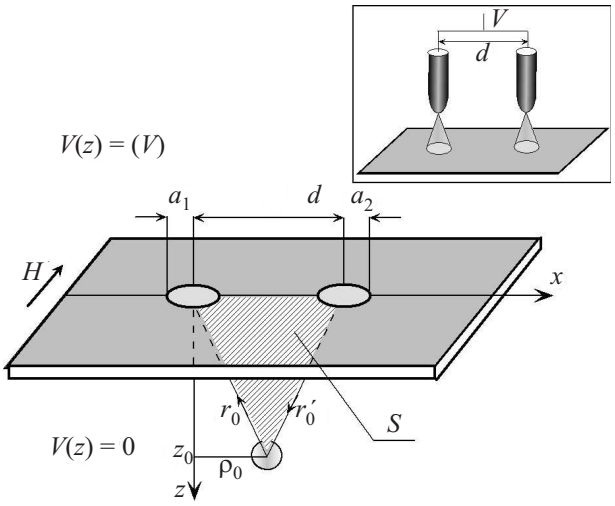

Fig. 1. Schematic arrangement of the system of two tunnel contacts, modelled as two orifices in an infinitely thin interface between conducting half-spaces. The inset shows the equivalent circuit with two STM tips, which provide the electron tunnelling paths through small areas with characteristic radii a_1 and a_2.

$$U(\mathbf{r}) = U_0 f(\boldsymbol{\rho})\delta(z). \tag{1}$$

In our case $f(\boldsymbol{\rho})$ describes two «windows» for electron tunneling and the reciprocal function $f^{-1}(\boldsymbol{\rho})$ can be presented as a sum of two terms

$$f^{-1}(\boldsymbol{\rho}) = \chi\left(\rho / a_1\right) + \chi\left(\left|\mathbf{d} - \boldsymbol{\rho}\right| / a_2\right), \qquad 2\pi\int_0^\infty dx x\chi(x) = 1, \tag{2}$$

where $\chi(x) \simeq 1$ for $x \lesssim 1$, and $\chi(x) \ll 1$ for $x \gg 1$, $a_{1,2}$ are the characteristic radii of the contacts, $\boldsymbol{\rho}$ is the component of the vector $\mathbf{r}$ parallel to the plane $z = 0$, $\mathbf{d}$ is a two-dimensional radius vector from the center of first contact to the center of second one. The absolute value d is the distance between contacts, assuming that this is smaller than the shortest relaxation length.

In the vicinity of the contacts a single defect is placed described a short range potential $D(\mathbf{r})$,

$$D(\mathbf{r}) = gD_0\left(\left|\mathbf{r} - \mathbf{r}_0\right|\right), \tag{3}$$

where g is the constant of interaction of the electrons with the defect, and $D_0(|\mathbf{r} - \mathbf{r}_0|)$ is a spherically symmetric function localized within a region of characteristic radius r_D centered at the point $\mathbf{r} = \mathbf{r}_0$, which satisfies the normalization condition

$$4\pi\int_0^\infty dr' r'^2 D_0(r') = 1. \tag{4}$$

For calculation of the conductance G we proceed as before. The probability density current is found by using the wave function $\psi(\mathbf{r})$ for the electrons tunnelling through the potential barrier in the plane of the orifices. The total electric current I in the system is calculated by integrations over electron momenta and over a real-space surface overlapping the contacts. We will take the temperature to be zero, and assume a small applied voltage V such that we stay in the linear regime of Ohm's law, $I = GV$. Under these assumptions the conductance G can be written as

$$G = \frac{e^2\hbar}{m^*}\nu(\varepsilon_F)\int\limits_{S_F, v_z>0} d\Omega_{\mathbf{p}} \int_S d\Omega r^2 \mathrm{Im}\left[\psi^*(\mathbf{r})\nabla\psi(\mathbf{r})\right]. \tag{5}$$

In Eq. (5) m^* is the effective electron mass, $\nu(\varepsilon_F)$ is the electron density of states at the Fermi level, $d\Omega$ and $d\Omega_{\mathbf{p}}$ are solid angles in the real and momentum spaces, respectively. As the surface for space integration we choose a half-sphere of radius r, larger than distance between the contacts d and centered at the center of first contact, $r = 0$, and covering the contacts in the lower half-space, $z > 0$. The integration over the directions of the momentum over the Fermi surface S_F is carried out for electrons tunnelling and having a positive projection v_z of the electron velocity on the contact axis z. As a consequence of the conservation of total current the integral over $d\Omega$ does not depend on the length we choose for the radius r.

The electron wave function $\psi(\mathbf{r})$ satisfies the Schrödinger equation

$$\left[\nabla^2 + \frac{2m^*}{\hbar^2}\left(\varepsilon - D(\mathbf{r})\right)\right]\psi(\mathbf{r}) = 0, \tag{6}$$

subject to the boundary conditions of continuity and of the jump of its derivative at $z = 0$. In Ref. 17 a solution of Eq. (6) was found for an arbitrary function $f(\boldsymbol{\rho})$, in the limit of weak tunnelling, $1/U_0 \to 0$, and for a purely ballistic contact (no defects present),

$$\psi_0(\boldsymbol{\rho}, z) = \frac{-ik_z\hbar^2}{(2\pi)^2 m^* U_0}\int\limits_{-\infty}^{\infty} d\boldsymbol{\varkappa}' e^{i\boldsymbol{\varkappa}'\boldsymbol{\rho}} e^{ik'_z z}\int\limits_{-\infty}^{\infty} d\boldsymbol{\rho}' \frac{e^{i(\boldsymbol{\varkappa}-\boldsymbol{\varkappa}')\boldsymbol{\rho}'}}{f(\boldsymbol{\rho}')}, \tag{7}$$

where $k'_z = \sqrt{\varkappa^2 + k_z^2 - \varkappa'^2}$, and $\boldsymbol{\varkappa}$ and k_z are the components of the vector $\mathbf{k}$ parallel and perpendicular to the interface, respectively. As a special case the authors of Ref. 17 considered a system of several orifices with different radii.

The characteristic radius of the region through which the electrons tunnel from the STM tip into the sample has sub-atomic size ($a \simeq 0.1$ Å) while the Fermi wave vector is $k_F \simeq 1\,\text{Å}^{-1}$. By using the condition $k_F\, a_{1,2} \ll 1$ we find, after integrating over $\boldsymbol{\varkappa}'$ in Eq. (7),

$$\psi_0(\mathbf{r}) = \frac{it(k_z)}{2}\left[(ka_1)^2\frac{z}{r}h_1^{(1)}(kr) + (ka_2)^2\frac{z}{r'}h_1^{(1)}(kr')e^{i\boldsymbol{\varkappa}\mathbf{d}}\right] \tag{8}$$

where $h_1^{(1)}(kr)$ is the spherical Bessel function of the first order, $r' = |\mathbf{r} - \mathbf{d}|$, and

$$t(k_z) = \frac{\hbar^2 k_z}{im^* U_0} \tag{9}$$

is the transmission amplitude of the electron wave function passing through a homogeneous barrier. Note that in the limit $k_F a_{1,2} \to 0$ the result of Eq. (8) does not depend on the concrete form of the function $\chi(\rho/a)$ in Eq. (2) and the wave function Eq. (8) as well as the conductance of the system are expressed in terms of the effective areas of the contacts, $\pi a_{1,2}^2$.

The effect of electron scattering by the short-range potential can be taken into account by the method proposed in Ref. 18. If the radius of action r_D of the potential $D(\mathbf{r})$ is of the order of Fermi wave length λ_F, in the region of the defect $|\mathbf{r} - \mathbf{r}_0| \lesssim r_D$ the wave function $\psi(\mathbf{r})$ can be taken as a constant $\psi(\mathbf{r}_0)$, as for a δ-function. Under this approximation Eq. (6) takes the form of a non-homogeneous equation with the right-hand member being $(2m^*/\hbar^2)D\psi(\mathbf{r}_0)$. In the limit $1/U_0 \to 0$ a solution of this equation can be expressed in terms of the solution of the homogeneous equation (see Eqs. (7), (8)) and the retarded electron Green's function of Eq. (6) for the semi-infinite half-space

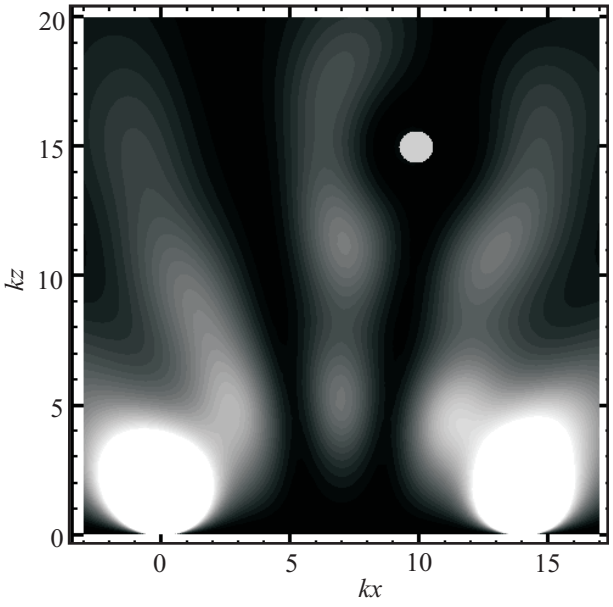

Fig. 2. Squared modulus of the wave function (10). The defect sits at $k\mathbf{r}_0 = (10, 0, 15)$, the distance between the contacts $kd = 14$, the scattering phase shift is $\delta_0 = 1.5$.

$$\psi(\mathbf{r}) = \psi_0(\mathbf{r}) + \frac{2m^*}{\hbar^2} T(k) \times$$

$$\times \left[G_0^{(+)}\left(|\mathbf{r} - \mathbf{r}_0|\right) - G_0^{(+)}\left(|\mathbf{r} - \tilde{\mathbf{r}}_0|\right) \right] \psi_0(\mathbf{r}_0), \qquad (10)$$

where $\tilde{\mathbf{r}}_0 = (\boldsymbol{\rho}_0, -z_0)$. $T(k)$ is the scattering matrix, which for a short-range scatterer can be expressed in terms of the s-wave scattering phase shift δ_0 [20]

$$T(k) = \frac{-\pi\hbar^2 (e^{2i\delta_0} - 1)}{m^* ik \left(1 + \frac{1}{4ikz_0} (e^{2i\delta_0} - 1) e^{2ikz_0} \right)}. \qquad (11)$$

The Green's function

$$G_0^{(+)}(x) = -\frac{\exp(ikx)}{4\pi x} \qquad (12)$$

is the retarded Green's function of a free electron. The phase shift δ_0 is determined by the scattering strength g as,

$$e^{i\delta_0} \sin\delta_0 = -\frac{m^* kg}{2\pi\hbar^2} \left(1 - \frac{8\pi m^* g}{\hbar^2} \int_0^\infty dr G_0^{(+)}(r) D(r) \right)^{-1}. \qquad (13)$$

Figure 2 illustrates the spacial variation of the wave function (10) for the case when the contacts and the scatterer are all placed in the plane $y = 0$. The interference of election waves passing through different contacts and their interference with the waves scattered by the defect are clearly visible. In order to make the effects more visible we used in Fig. 2 a large value for the scattering phase $\delta_0 = 1.5$, which is acceptable only for Kondo resonance scattering by a magnetic impurity (see, for example, [19]). The grey circle round the point $\mathbf{r} = \mathbf{r}_0$ in Fig. 2 is the region in which the Eq. (10) is not valid because of divergence of the Green function.

Substituting the wave function (10) into the general expression for the conductance G (5) we find

$$G = G_c(a_1, a_2) + G_{\text{osc}}, \qquad (14)$$

where G_c is the conductance of the double contact system in the absence of the defect

$$G_c(a_1, a_2) = G_0(a_1) + G_0(a_2) + G_{12}, \qquad (15)$$

G_0 is an inherent conductance of the single contact [17]

$$G_0(a) = |t(k_F)|^2 \frac{e^2 (k_F a)^4}{36\pi\hbar}, \qquad (16)$$

and G_{12} takes into account the interference of electron waves passing through different contacts

$$G_{12} = |t(k_F)|^2 \frac{e^2 (k_F a_1)^2 (k_F a_2)^2}{18\pi\hbar} f^2(k_F d). \qquad (17)$$

Here we introduced the notation

$$f(x) = \frac{3 j_1(x)}{x}, \qquad (18)$$

$j_1(x)$ the spherical Bessel function of the first kind such that $f(0) = 1$. The second term in Eq.(14), G_{osc}, describes the quantum interference resulting from the scattering of the electrons by the defect

$$G_{\text{osc}}(r_0, d) = G_0(a_1)\Gamma(\mathbf{r}_0) + G_0(a_2)\Gamma(\mathbf{r}_0') +$$

$$+ 2G_{12}\Psi(\mathbf{r}_0, \mathbf{r}_0') / f(k_F d), \qquad (19)$$

where $\mathbf{r}_0' = (\boldsymbol{\rho}_0 - \mathbf{d}, z_0)$, and r_0' is the distance between the defect and the second contact. The functions $\Gamma(\mathbf{r}_0)$ and $\Gamma(\mathbf{r}_0')$ take into account the effect of interference of electron waves passing through the contact and returning to the same contact after scattering by the defect,

$$\Gamma(\mathbf{r}) = \frac{1}{F(z)} \sin\delta_0 \frac{z^2}{r^2} [12 j_1(k_F r)\gamma(k_F r) +$$

$$+ 6(1 - j_0(2k_F z))(k_F r)^{-4} ((kr)^2 + 1)\sin\delta_0], \qquad (20)$$

where

$$F(z) = 1 + 2\sin\delta_0 \times$$

$$\times \left[\left(\frac{1}{2(2k_F z)^2} - j_0(2k_F z) \right) \sin\delta_0 - y_0(2k_F z)\cos\delta_0 \right], \qquad (21)$$

and

$$\gamma(\mathbf{r}) = -y_1(k_F r)\cos\delta_0 + \sin\delta_0 [j_1(k_F r)(j_0(2k_F z) - 1) +$$

$$+ y_0(2k_F z) y_1(k_F r)]. \qquad (22)$$

In the last term in Eq. (19) $\Psi(\mathbf{r}_0, \mathbf{r}_0')$ describes the interference of electron waves that arrive at the other contact after scattering by the defect,

$$\Psi(\mathbf{r}, \mathbf{r}') = F^{-1} \sin\delta_0 \frac{z^2}{rr'} [j_1(k_F r')\gamma(\mathbf{r}) + j_1(k_F r)\gamma(\mathbf{r}') +$$

$$+ \sin\delta_0 (j_0(k_F d) - j_0(k_F \sqrt{4z^2 + d^2})) \times$$

$$\times (j_1(k_F r) j_1(k_F r') - y_1(k_F r) y_1(k_F r'))]. \qquad (23)$$

For $a_2 = 0$ (i.e., when we have just a single contact) Eq. (14) coincides with the expression for the conductance of a tunnel point contact obtained in Ref. 20. Figure 3 illustrates the dependence of the oscillatory part of the conductance (19) on the position of the defect in the plane $z = z_0$. The oscillatory pattern presented in Fig. 3

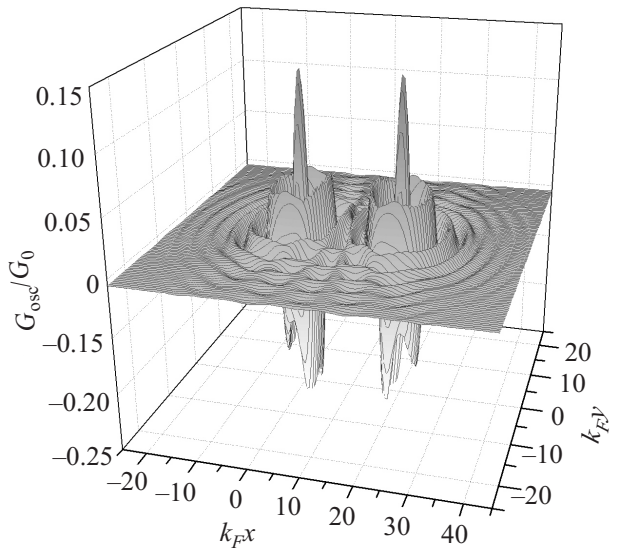

Fig. 3. Dependence of the normalized oscillatory part of the conductance $G_{\rm osc}/G_0$ as a function of the defect position ρ_0 in the plane parallel to interface $z=0$, $k_Fz_0=5$. The distance between the contacts is taken as $k_Fd=20$, and the scattering phase shift is $\delta_0=1.5$.

represents an image which could be obtained by DSTM when mapping the tunnelling conductance in the vicinity of the subsurface defect.

The general formula for the conductance (14) can be simplified for large distances between the contacts and the defect, $r_0, r_0' \gg 1/k_F$, and for a weak scattering potential $\delta_0 \simeq -gm^*k_F/2\pi\hbar^2 \ll 1$. Under these assumptions the normalized oscillatory part of the conductance, in the linear approximation in g, can be written as

$$\frac{G_{\rm osc}}{G_0} = -6\delta_0\frac{z_0^2}{k_F^2}\left\{\frac{1}{r_0^4}\sin 2k_Fr_0 + \frac{1}{r_0'^4}\sin 2k_Fr_0' - \right.$$
$$\left. -\frac{2f(k_Fd)}{(r_0r_0')^2}\sin k_F(r_0+r')\right\}. \qquad (24)$$

For simplicity we take here $a_1 = a_2 = a$. Equation (24) shows that in contrast to one tunnel point contact, for which $G_{\rm osc}\sim\sin 2k_Fr_0$ when $k_Fr_0\gg 1$, the oscillatory dependence of the double contact has a phase shift ϑ that depends on the distance between the contacts

$$\frac{G_{\rm osc}}{G_0}\sim\sin(2k_Fr_0+\vartheta), \qquad (25)$$

where

$$\vartheta(\rho_0,z_0,d) = -\arcsin\left[\frac{\sin 2\varphi + 2f(k_Fd)\sin\varphi}{\sqrt{2+4f^2(k_Fd)+4f(k_Fd)(\cos 2\varphi+2\cos\varphi)}}\right], \quad d\ll r_0, \qquad (26)$$

and $\varphi = k_F\rho_0 d/r_0$. The defect position in the plane parallel to the surface, ρ_0, is known from the interference pattern of the conductance oscillations (see Fig. 3). In principle, the depth of the defect z_0 may be found from the experimental data in the following way: changing the distance between the contacts over a small range $\Delta d \ll d$ leads to the appearance of an additional phase shift $\Delta\vartheta(\rho_0,z_0,d)$, which can be defined from the dependence $G_{\rm osc}(\rho_0,z_0,d)$, see Fig. 4. The depth z_0 can be obtained as a numerical solution of the equation

$$\Delta\vartheta = \vartheta_d'(\rho_0,z_0,d)\Delta d. \qquad (27)$$

Let us now consider applying a magnetic field **H** parallel to the surface of the sample (see Fig. 1). If the external magnetic field is sufficiently weak, such that the radius of the electron trajectories $r_H = \hbar ck_F/eH$ is much larger than the distances between the contacts and the impurity, r_0, r_0', the magnetic distortions of the trajectories [21] are negligible, i.e., the trajectories can be considered as straight lines.

Under this condition of $r_H \gg r_0$, r_0', the zero-field wave-function $\psi(\mathbf{r})$ acquires an additional phase:

$$\tilde\psi(\mathbf{r}) = \psi(\mathbf{r})\exp\left(\frac{ie}{c\hbar}\int_0^{\mathbf{r}}\mathbf{A}(\mathbf{r}'')d\mathbf{r}''\right), \qquad (28)$$

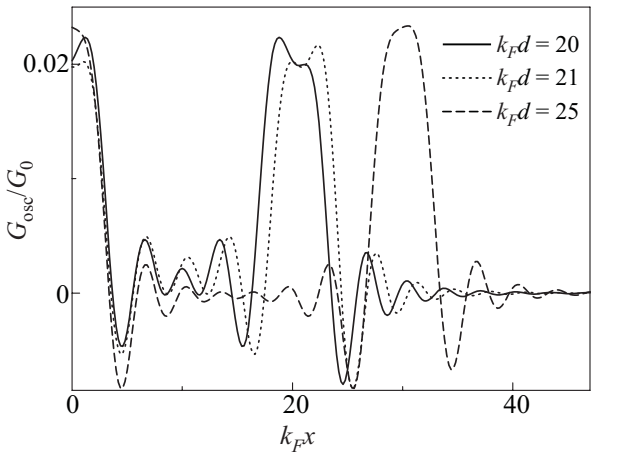

Fig. 4. Dependencies of the oscillatory part of the conductance on the coordinate x_0 of the defect for different distances between the contacts, for $y_0=0$, $k_Fz_0=5$, and $\delta_0=0.1$.

and the Green function similarly takes the form [16]:

$$\tilde{G}(\mathbf{r},\mathbf{r}_0) = G(\mathbf{r},\mathbf{r}_0)\exp\left(\frac{ie}{c\hbar}\int\limits_{\mathbf{r}_0}^{\mathbf{r}}\mathbf{A}(\mathbf{r}'')d\mathbf{r}''\right). \qquad (29)$$

Here, $\mathbf{A}(\mathbf{r})$ is the vector potential of the magnetic field.

On account of this change in the wave function (28) the formula for the conductance G is modified and takes the form:

$$G = G_c(a_1,a_2) + \tilde{G}_{\rm osc}(r_0,d,H), \qquad (30)$$

$$\tilde{G}_{\rm osc}(r_0,d,H) = G_0(a_1)\Gamma(\mathbf{r}_0) + G_0(a_2)\Gamma(\mathbf{r}_0') + 2G_{12}\tilde{\Psi}(\mathbf{r}_0,\mathbf{r}')/f(k_F d), \qquad (31)$$

$$\tilde{\Psi}(\mathbf{r},\mathbf{r}') = \frac{1}{F}\sin\delta_0\frac{z^2}{r'}\left[j_1(k_F r')\left(\gamma(\mathbf{r})\cos\frac{\pi\Phi}{\Phi_0}+\tilde{\gamma}(\mathbf{r})\sin\frac{\pi\Phi}{\Phi_0}\right)+j_1(k_F r)\left(\gamma(\mathbf{r}')\cos\frac{\pi\Phi}{\Phi_0}+\tilde{\gamma}(\mathbf{r}')\sin\frac{\pi\Phi}{\Phi_0}\right)+\right.$$

$$\left.+\sin\delta_0\left(j_0(k_F d)-j_0(k_F\sqrt{4z^2+d^2}\,)\right)\left(j_1(k_F r)j_1(k_F r')-y_1(k_F r)y_1(k_F r')\right)\right], \qquad (32)$$

$$\tilde{\gamma}(\mathbf{r}) = \cos\delta_0 j_1(k_F r)+\sin\delta_0\left\{y_1(k_F r)\left(j_0(2k_F z)-1\right)-y_0(2k_F z)j_1(k_F r)\right\}, \qquad (33)$$

where $\gamma(\mathbf{r})$ is defined by (22), $\Phi_0 = \pi c\hbar/e$ is the flux quantum and $\Phi = \mathbf{HS}$ is the magnetic flux through the triangle formed by vectors $\mathbf{r}_0$, $\mathbf{r}_0'$, and the vector $\mathbf{d}$ connecting the contacts. At $H = 0$ the expression (30) reduces to the formula obtained earlier (14).

At $r_0 \gg 1/k_F$, and $\delta_0 \ll 1$, Eq. (31) takes the form

$$\frac{\Delta G_{\rm osc}(r_0,d,H)}{G_0} \simeq -\frac{12\delta_0 z_0^2 f(k_F d)}{k_F^2 (r_0 r_0')^2}\times$$

$$\times\left[\cos k_F r_0 \sin\left(k_F r_0' - \frac{\pi\Phi}{\Phi_0}\right)+\cos k_F r_0' \sin\left(k_F r_0 - \frac{\pi\Phi}{\Phi_0}\right)\right]. \qquad (34)$$

Similar oscillations in the electron local density of states have been predicted in Ref. 22 for a system of two adatoms and an STM tip in a plane perpendicular to a surface magnetic field.

If the period of the oscillations is known, the depth z_0 can be determined using the following procedure: In the most convenient geometry of the experiment the contacts should be placed so that the vectors $\mathbf{r}_0$, $\mathbf{r}_0'$ and the normal to the sample surface are situated in the same plane, i.e., the vectors $\mathbf{H}$ and $\mathbf{S}$ are parallel. For our illustration in Fig. 1 that means the coordinate $\boldsymbol{\rho}_0$ of the defect in the plane xy is on the line connecting the tips. In this case the relation between the period of oscillations ΔH and the depth z_0 is very simple

$$z_0 = \frac{4\Phi_0}{d\Delta H}. \qquad (35)$$

Note that observation of the conductance oscillations (34) requires a sufficiently strong magnetic field. Currently in low temperature STM the magnetic field up to 15 T is reachable [23]. For example, in order to observe the quote of period ΔH for $z_0 = d = 20$ nm it is necessary to apply the field $H =$ 5 T. For typical metals, for which $\lambda_F \sim 0.1$ nm, for the distance between the contacts and the defect $r_0 \gtrsim 10$ nm the amplitude of conductance oscillations become very small $G_{\rm osc} \sim G_0(\lambda_F/r_0)^2 \sim (10^{-4}\text{–}10^{-5})G_0$. Therefore more suitable objects for application of proposed magnetic method of determination of the defect position below the surface are semiconductors, semimetals (Bi, Sb and their ordered alloys) where the Fermi wave length $\lambda_F \sim 10$ nm. Also the large amplitude $G_{\rm osc} \sim (10^{-2}\text{–}10^{-3})G_0$ could be expected in the metals of the first group, a Fermi surface of which has small cavities with effective mass $m^* \simeq (10^{-2}\text{–}10^{-3})m_0$ (m_0 is the mass of a free electron). As well a low temperature STM should be used to avoid electron-phonon scattering on the electron trajectory.

Thus, in this paper we have investigated theoretically the conductance of the system consisting of two close tunnel point contacts in the vicinity of which the point defect is situated. In approximation of *s*-wave scattering which is valid for short range scattering potential the oscillatory dependence of conductance on the separation between the contacts and their distances from the defect is studied. We proposed an alternative way that allows to determine the depth of the subsurface impurity by measuring the phase change in the conductance oscillation, arising when we change the distance between the contacts of double-tip STM. Also it was obtained that for the case when low magnetic field which is parallel to the surface of the sample the depth of the subsurface impurity can be easily found from the period of Aharonov–Bohm type oscillations of conductance, which arise in this case.

1. P. Jasninsky, P. Coenen, G. Pirug, and B. Voigtlander, *Rev. Sci. Instrum*. **77**, 093701 (2006).
2. H. Okamoto and D. Chen, *Rev. Sci. Instrum*. **72**, 4398 (2001).
3. W. Yi, I.I. Kaya, I.B. Altfeder, I. Appelbaum, D.M. Chen, and V. Narayanamurti, *Rev. Sci. Instrum*. **76**, 063711 (2005).
4. H. Grube, B.C. Harrison, J. Jia, and J.J. Boland, *Rev. Sci. Instrum*. **72**, 4388 (2001).
5. M.E. Flatte and J.M. Byers, *Phys. Rev*. **B53**, 10536(R) (1996).
6. P. Jaschinsky, J. Wensorra, M.I. Lepsa, J. Mysliveček, and B. Voigtlander, *J. Appl. Phys*. **104**, 094307 (2008).
7. J.M. Byers and M.E. Flatte, *Phys. Rev. Lett*. **74**, 306 (1995).
8. Q. Niu, M.C. Chang, and C.K. Shih, *Phys. Rev*. **B51**, 5502 (1995).
9. R. Dana, I. Kiruschev, P.D. Tran, P. Doppelt, and Y. Manassen, *Israel J. Chem*. **48**, 87 (2008).
10. Ye.S. Avotina, Yu.A. Kolesnichenko, and J.M. van Ruitenbeek, *Fiz. Nizk. Temp*. **36**, 1066 (2010) [*Low Temp. Phys*. **36**, Nos. 10–11 (2010)].
11. K. Kobayashi, *Phys. Rev*. **B54**, 17029 (1996).
12. Ye.S. Avotina, Yu.A. Kolesnichenko, A.N. Omelyanchouk, A.F. Otte, and J.M. van Ruitenbeek, *Phys. Rev*. **B71**, 115430 (2005).
13. Ye.S. Avotina, Yu.A. Kolesnichenko, A.F. Otte, and J.M. van Ruitenbeek, *Phys. Rev*. **B74**, 085411 (2006).
14. Ye.S. Avotina, Yu.A. Kolesnichenko, S.B. Roobol, and J.M. van Ruitenbeek, *Fiz. Nizk. Temp*. **34**, 268 (2008) [*Low Temp. Phys*. **34**, 207 (2008)].
15. A. Wiesmann , M. Wenderoth, S. Lounis, P. Zahn, N. Quaas, R.G. Ulbrich, P.H. Dederichs, and S. Blugel, *Science* **323**, 1190 (2009).
16. A. Cano and I. Paul, *Phys. Rev*. **B80**, 153401 (2009).
17. I.O. Kulik, Yu.N. Mitsai, and A.N. Omelyanchouk, *Zh. Eksp. Theor. Phys*. [*Sov. Phys. JETP*] **63**, 1051 (1974).
18. E. Granot and M.Ya. Azbel, *Phys. Rev*. **B50**, 8868 (1994); *J. Phys.: Condens. Matter* **11**, 4031 (1999).
19. A.A. Abrikosov, *Fundamentals of the Theory of Metals*, North Holland (1988).
20. Ye.S. Avotina, Yu.A. Kolesnichenko, and J.M. van Ruitenbeek, *J. Phys: Condens. Matter* **20**, 115208 (2008).
21. Ye.S. Avotina, Yu.A. Kolesnichenko, A.F. Otte, and J.M. van Ruitenbeek, *Phys. Rev*. **B75**, 125411 (2007).
22. A. Cano and I. Paul, *Phys. Rev*. **B80**, 153401 (2009).
23. V. Shvarts, Z. Zhao, L. Bobb, and M. Jirmanus, *J. Phys.: Conf. Ser*. **150**, 012046 (2009).